

Measurement of the rare decay $\pi^0 \rightarrow e^+e^-$

E. Abouzaid,⁴ M. Arenton,¹¹ A. R. Barker,^{5,*} L. Bellantoni,⁷ A. Bellavance,⁹ E. Blucher,⁴ G. J. Bock,⁷ E. Cheu,¹ R. Coleman,⁷ M. D. Corcoran,⁹ B. Cox,¹¹ A. R. Erwin,¹² C. O. Escobar,³ A. Glazov,⁴ A. Golossanov,¹¹ R. A. Gomes,³ P. Gouffon,¹⁰ K. Hanagaki,⁸ Y. B. Hsiung,⁷ H. Huang,⁵ D. A. Jensen,⁷ R. Kessler,⁴ K. Kotera,⁸ A. Ledovskoy,¹¹ P. L. McBride,⁷ E. Monnier,^{4,†} K. S. Nelson,¹¹ H. Nguyen,⁷ R. Niclasen,⁵ D. G. Phillips II,¹¹ H. Ping,¹² X. R. Qi,⁷ E. J. Ramberg,⁷ R. E. Ray,⁷ M. Ronquest,¹¹ E. Santos,¹⁰ J. Shields,¹¹ W. Slater,² D. Smith,¹¹ N. Solomey,⁴ E. C. Swallow,^{4,6} P. A. Toale,⁵ R. Tschirhart,⁷ C. Velissaris,¹² Y. W. Wah,⁴ J. Wang,¹ H. B. White,⁷ J. Whitmore,⁷ M. J. Wilking,⁵ B. Winstein,⁴ R. Winston,⁴ E. T. Worcester,⁴ M. Worcester,⁴ T. Yamanaka,⁸ E. D. Zimmerman,^{5,‡} and R. F. Zukanovich¹⁰

¹University of Arizona, Tucson, Arizona 85721

²University of California at Los Angeles, Los Angeles, California 90095

³Universidade Estadual de Campinas, Campinas, Brazil 13083-970

⁴The Enrico Fermi Institute, The University of Chicago, Chicago, Illinois 60637

⁵University of Colorado, Boulder, Colorado 80309

⁶Elmhurst College, Elmhurst, Illinois 60126

⁷Fermi National Accelerator Laboratory, Batavia, Illinois 60510

⁸Osaka University, Toyonaka, Osaka 560-0043 Japan

⁹Rice University, Houston, Texas 77005

¹⁰Universidade de São Paulo, São Paulo, Brazil 05315-970

¹¹The Department of Physics and Institute of Nuclear and Particle Physics, University of Virginia, Charlottesville, Virginia 22901

¹²University of Wisconsin, Madison, Wisconsin 53706

(Dated: August 8, 2018)

The branching ratio of the rare decay $\pi^0 \rightarrow e^+e^-$ has been measured precisely, using the complete data set from the KTeV E799-II experiment at Fermilab. We observe 794 candidate $\pi^0 \rightarrow e^+e^-$ events using $K_L \rightarrow 3\pi^0$ as a source of tagged π^0 s. The expected background is 52.7 ± 11.2 events, predominantly from high e^+e^- mass $\pi^0 \rightarrow e^+e^-\gamma$ decays. We have measured $B(\pi^0 \rightarrow e^+e^-, (m_{e^+e^-}/m_{\pi^0})^2 > 0.95) = (6.44 \pm 0.25_{\text{stat}} \pm 0.22_{\text{syst}}) \times 10^{-8}$, which is above the unitary bound from $\pi^0 \rightarrow \gamma\gamma$ and within the range of theoretical expectations from the standard model.

I. INTRODUCTION

In this report we present a new measurement of the $\pi^0 \rightarrow e^+e^-$ branching ratio using a larger data set from KTeV-E799 at Fermilab. This result used all data taken in the two runs of the experiment (1997 and 1999-2000). It supersedes the previously published measurement [1] from KTeV-E799, which used only the 1997 data. The basic measurement technique of using $K_L \rightarrow 3\pi^0$ as a source of tagged π^0 decays is adapted from the previous analysis.

A. The Decay $\pi^0 \rightarrow e^+e^-$

The rare decay $\pi^0 \rightarrow e^+e^-$ proceeds, to lowest order, in a one-loop process via a two-photon intermediate state. The decay rate was first predicted by Drell [2] and has since received considerable attention both theoretically

and experimentally. Relative to the $\pi^0 \rightarrow \gamma\gamma$ rate, it is suppressed by two powers of α and is further suppressed by $2(m_e/m_{\pi^0})^2$ due to the approximate helicity conservation of the interaction. The lowest order contribution has been calculated exactly in terms of a form factor [3], and lowest order radiative corrections have been calculated [4]. The contribution to the rate from on-shell photons is model independent and can be calculated exactly to form a lower “unitary bound” [5] on the branching ratio, $B(\pi^0 \rightarrow e^+e^-) \geq 4.69 \times 10^{-8}$, neglecting radiative corrections.

The primary interest in the decay rate is the excess above the unitary bound, as this is the contribution from virtual photons. Attempts to model the form factor and make predictions for the off-shell photon contribution have been made, most successfully using vector meson dominance (VMD) and chiral perturbation theory (χ PT) approaches [6, 7, 8, 9]. A new measurement is significant for χ PT, where $\pi^0 \rightarrow e^+e^-$ represents a tight experimental constraint on calculations. It is of particular interest because $\pi^0 \rightarrow e^+e^-$ is the best-measured decay of a pseudoscalar meson to a lepton pair and has no significant contributions from short-distance physics. Constraints on χ PT from $\pi^0 \rightarrow e^+e^-$ can be used to improve predictions for other $P^0 \rightarrow l^+l^-$ decays, including $\eta \rightarrow \mu^+\mu^-$ and the long-distance contribution to $K_L^0 \rightarrow \mu^+\mu^-$. The

*Deceased.

†Permanent address C.P.P. Marseille/C.N.R.S., France

‡To whom correspondence should be addressed. Electronic address: edz@colorado.edu

smaller short-distance contribution to $K_L^0 \rightarrow \mu^+\mu^-$ is dominated by a top-quark loop and thus is a potential source of information on $|V_{td}|$ if the long-distance contribution can be subtracted successfully.

Earlier interest in $\pi^0 \rightarrow e^+e^-$ was due to experimental indications [10, 11] that the decay rate could be substantially higher than predicted, indicating possible new physics. Later experiments [12, 13, 14] obtained results more consistent with the standard model predictions, and the most recent result from KTeV-E799 [1] provided a precise measurement of the branching ratio falling entirely within the standard model prediction.

II. THE KTeV-E799 EXPERIMENT

The KTeV facility (Figure 1) at Fermilab was a general-purpose neutral kaon beam and decay spectrometer. It was operated for two experiments: E832, which used an active regenerator to produce a K_S flux for measuring $\Re(\epsilon'/\epsilon)$, and E799-II, which had a higher intensity K_L flux and performed searches and measurements for a variety of rare K_L decays. The analysis described here uses E799-II data.

A. The kaon beam

At KTeV, 800 GeV protons hit a BeO target and produced two nearly parallel neutral beams that were defined by sweeper magnets and collimators. A vacuum decay volume was located from 94 to 158 meters downstream of the target. In this region, the beams consisted of K_L^0 and neutrons, with small numbers of shorter-lived neutral hyperons and K_S^0 remaining. The K_L^0 energies in this region ranged from 20–200 GeV. The decay region ended at a Mylar-Kevlar vacuum window which was followed by a charged particle spectrometer.

B. The charged spectrometer

Charged tracks were detected by four drift chambers separated by 6 m, 9 m, and 6 m. A momentum analysis dipole magnet sat between the second and third chambers. The field integral from the magnet was 205 MeV/c in the 1997 run period and 150 MeV/c in 1999. The momentum resolution of the spectrometer in the range of interest was 0.9%. A set of transition radiation detectors (TRDs) was placed after the the last drift chamber. This detector provided particle identification used to distinguish electrons from pions but was not needed in this analysis because there were no significant non-electron backgrounds. Following the TRDs there was a segmented array of scintillator planes for fast triggering on events with charged particles.

C. Photon and muon detection

The final detector for electromagnetic particles was a calorimeter consisting of 3100 pure CsI crystals. The crystal blocks were arranged in a 1.8×1.8 m² square array with two 15×15 cm² holes near the middle for the neutral beams to pass through. The crystals were 27 radiation lengths deep, which contained nearly all electromagnetic showers. The energy resolution for electromagnetic particles was $(0.45 \oplus 2.0/\sqrt{E})\%$, where E is the energy in GeV and the addition is in quadrature. The perimeters of the vacuum decay region, spectrometer, and calorimeter were instrumented with a total of nine lead-scintillator photon veto counters to reject particles escaping the detector at high angles. Two vetoes were also used around the edges of the two beam holes in the calorimeter. Downstream of the calorimeter, a 15 cm lead wall showered remaining hadrons and the showers were detected by a scintillator plane in order to reject events with hadrons in the final state. Behind an additional 4 m of steel was a muon veto system, which was used to detect decays with muons in the final state. For a more complete discussion of the KTeV detector see Ref. [15].

III. DATA COLLECTION AND ANALYSIS

The $\pi^0 \rightarrow e^+e^-$ branching ratio was found by normalizing signal candidates to $\pi^0 \rightarrow e^+e^-\gamma$ (Dalitz decays) with $m_{e^+e^-} > 65$ MeV/ c^2 . Both samples were from $K_L \rightarrow 3\pi^0$ decays where the other two π^0 's in the event decayed to $\gamma\gamma$. This normalization mode was selected because its final state particles and kinematics are similar to the signal, allowing many detector response systematic effects to cancel.

A. Trigger requirements

The trigger for both signal and normalization required activity in the chambers consistent with two tracks, plus total energy in the calorimeter above 25 GeV and at least four separate energy clusters in the calorimeter where at least one crystal in the cluster had more than 1 GeV of energy. The trigger also required no significant energy in either the photon veto counters or the hadron anti. Signal and normalization candidates were collected, reconstructed, and analyzed in parallel.

B. Radiative corrections

The presence of internal bremsstrahlung off the electrons in $\pi^0 \rightarrow e^+e^-$ complicates the analysis, because the final state contains the same particles as the tree-level Dalitz decay $\pi^0 \rightarrow e^+e^-\gamma$ (though the two decays generally populate different regions of phase space). The

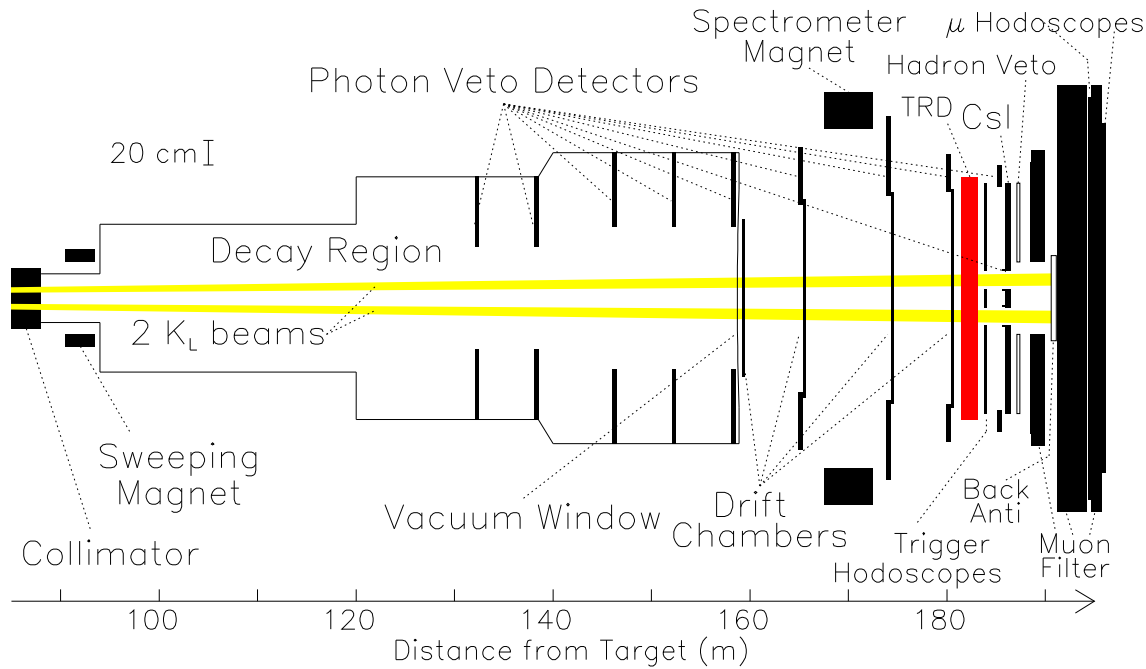


FIG. 1: The KTeV spectrometer in E799-II configuration.

signal must therefore be defined as a region where radiation is soft and where there is little contribution from the Dalitz decay. Following the conventions of Ref. [1, 14], we defined the signal by requiring Dalitz $x_D \equiv (m_{e^+e^-}/m_{\pi^0})^2 > 0.95$, considering the rest of the spectrum as background. This definition left very little intrinsic background from the Dalitz decays while including 89% of the $\pi^0 \rightarrow e^+e^-$ bremsstrahlung spectrum. Also, in this region the quantum mechanical interference between the two modes is negligible [4]. In addition to the inner bremsstrahlung diagram, a virtual photon correction suppresses the total $\pi^0 \rightarrow e^+e^-$ decay rate by 3.4%. Both effects must be accounted for in comparing the measured decay rate with theoretical models that neglect radiation.

The experimentally measured quantity was the ratio:

$$\frac{\Gamma(\pi^0 \rightarrow e^+e^-, x_D > 0.95)}{\Gamma(\pi^0 \rightarrow e^+e^-\gamma, x_D > 0.232)} \quad (1)$$

where the $\pi^0 \rightarrow e^+e^-\gamma$ rate is inclusive of $\pi^0 \rightarrow e^+e^-\gamma\gamma$ as calculated from lowest-order radiative corrections [16].

C. Reconstruction and event selection

For both modes the full $K_L \rightarrow 3\pi^0$ decay chain was reconstructed. Signal events had 6 electromagnetic clusters and 2 oppositely charged tracks, while the normalization had 7 clusters and 2 tracks. The tracks in both modes also had to be electron candidates, defined to be the case

when a track of momentum p pointed to a calorimeter cluster of energy E and $|E/p - 1| \leq 0.08$. The total energy in the calorimeter was required to be above 35 GeV and each cluster energy above 1.75 GeV.

D. Photon and vertex reconstruction

Clusters with no tracks pointing to them were assumed to be photons coming from π^0 decays. For $\pi^0 \rightarrow e^+e^-$ candidates, the four photons could be assigned in three possible pairing combinations, while for $\pi^0 \rightarrow e^+e^-\gamma$ candidates there were 15 pairing combinations for the five photons. The best pairing was found using the following procedure: For each pair of photons the distance d from the calorimeter to the decay vertex was calculated assuming the pair originated from a $\pi^0 \rightarrow \gamma\gamma$ decay: $d = r_{12}\sqrt{E_1E_2}/m_{\pi^0}$, where r_{12} was the distance between the two photon clusters and E_1 and E_2 were the cluster energies. The z -position of the decay vertex was then $z = z_{\text{CsI}} - d$. A pairing χ^2 was calculated for the hypothesis that the two decay positions (z_1 and z_2) coincided with each other and with the decay vertex obtained from the electron tracks (z_{ee}):

$$\chi^2 = \frac{(z_1 - \bar{z})^2}{\sigma^2(z_1)} + \frac{(z_2 - \bar{z})^2}{\sigma^2(z_2)} + \frac{(z_{ee} - \bar{z})^2}{\sigma^2(z_{ee})}. \quad (2)$$

For each pairing case, the mean decay position \bar{z} was found by minimizing the χ^2 . The pairing with the smallest minimum χ^2 was selected and the obtained decay

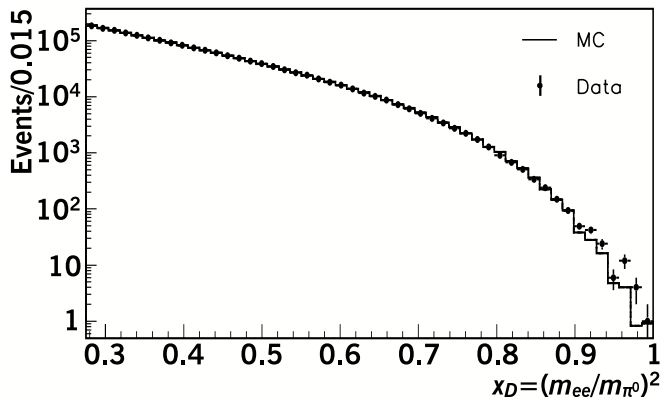


FIG. 2: Dalitz $x_D \equiv (m_{e^+e^-}/m_{\pi^0})^2$ for fully-reconstructed Dalitz decay candidates after normalization mode analysis cuts. Monte Carlo prediction using the world average form factor slope parameter is overlaid.

vertex z -position, \bar{z} , was then used to reconstruct particle trajectories. This decay vertex calculation combined information from the calorimeter and drift chambers to optimize the overall resolution on the vertex position. The vertex was required to be $96 \leq \bar{z} \leq 158$ m downstream of the target, removing events near the ends of the decay region.

E. Final sample selection

For $\pi^0 \rightarrow e^+e^-$ candidates, the reconstructed kaon mass was required to be between 490–510 MeV/ c^2 . For normalization $\pi^0 \rightarrow e^+e^-\gamma$ candidates, where backgrounds were low and event reconstruction was poorer due to the additional pairing ambiguity, the allowed interval was 475–525 MeV/ c^2 . The total reconstructed momentum transverse to the incident kaon direction, defined as the line between the center of the target and the decay vertex, was required to be $p_{\perp}^2 < 10^{-3}$ GeV $^2/c^2$. For the normalization sample the reconstructed Dalitz decay mass $m_{e^+e^-\gamma}$ was required to be in the interval 100–200 MeV/ c^2 , with an additional requirement that the reconstructed electron pair mass $m_{e^+e^-}$ be greater than 70 MeV/ c^2 . This last requirement removed resolution effects near the 65 MeV/ c^2 cutoff.

A detailed description of the detector and beamline was implemented in a Monte Carlo (MC) simulation, which was used to study detector geometry, acceptance, and backgrounds. The decay simulation included $\mathcal{O}(\alpha)$ radiative corrections to $\pi^0 \rightarrow e^+e^-$ based on the work of Bergström [4], while for $\pi^0 \rightarrow e^+e^-\gamma$, the world average form factor slope [17] and radiative corrections to order $\mathcal{O}(\alpha^2)$ [16] were used. Figure 2 shows the distribution of x_D for the normalization Dalitz-decay sample in both data and MC.

Beyond the basic reconstruction requirements above, additional cuts were needed to remove backgrounds to $\pi^0 \rightarrow e^+e^-$. The full reconstruction of the K_L decay

chain removed all significant backgrounds except those originating from $K_L \rightarrow 3\pi^0$ decays. One category of backgrounds was $K_L \rightarrow 3\pi^0$ decays with four electrons in the final state, where two were lost and the remaining two mimicked the $\pi^0 \rightarrow e^+e^-$ decay. Low-energy electrons could be swept out of the fiducial region by the analysis magnet, never making a complete track. One major source of this background was $K_L \rightarrow 3\pi^0 \rightarrow (e^+e^-\gamma) + (e^+e^-\gamma) + (\gamma\gamma)$, where the photons from the Dalitz decays were accidentally reconstructed as a $\pi^0 \rightarrow \gamma\gamma$ decay. Another source was the rarer decay $\pi^0 \rightarrow e^+e^-e^+e^-$. Finally, photons from π^0 decays could convert to e^+e^- pairs in the vacuum window just upstream of the chambers. Events with two of these conversions, or one in combination with a Dalitz decay, also contributed to four-track background.

Backgrounds in which the two electrons came from different π^0 s were reduced by a requirement on the pairing χ^2 defined above: a cut of $\chi^2 < 20$ was used in both the signal and the normalization mode. To reduce the four-electron backgrounds further, a cut on evidence for extra in-time activity in the second drift chamber was made. Removing events with in-time activity in the second drift chamber more than 0.5 cm away from any reconstructed track reduced the four-track backgrounds to 0.7% of the expected signal. The effect of this cut on the signal (and any backgrounds without extra charged particles) was an overall reduction of 7.7% in acceptance. Both of these background cuts were also used in the Dalitz normalization sample in order to cancel systematic effects associated with modeling the cut efficiency.

F. Background and systematic error estimation

After all cuts were applied, the largest remaining background came from high $m_{e^+e^-}$ Dalitz decays where the Dalitz photon was lost and the e^+e^- mass was reconstructed 0–0.5 MeV/ c^2 high.

A plot of $m_{e^+e^-}$ after all cuts, Fig. 3, shows the signal peak at the π^0 mass and a background distribution that extends under the peak. The background MC normalized by the measured number of sideband Dalitz decays is plotted as well. The signal region was $131.6 < m_{e^+e^-} < 138.4$ MeV/ c^2 , in which 794 events were found. The MC predicted a 2.94% detector acceptance for the signal in the 1997 run period and 3.14% in 1999. In the normalization sample, 1 874 637 candidates were found with 0.1% background. The acceptance for the normalization was 1.21% in 1997 and 1.38% in 1999. The background in the signal region was estimated using a MC simulation of each of the considered backgrounds. Of these background events, 79% were high e^+e^- -mass Dalitz decays and the remainder were four-electron final states.

The important systematic error sources that were identified are listed in Table I. External systematic errors are separated so the result may be corrected in the fu-

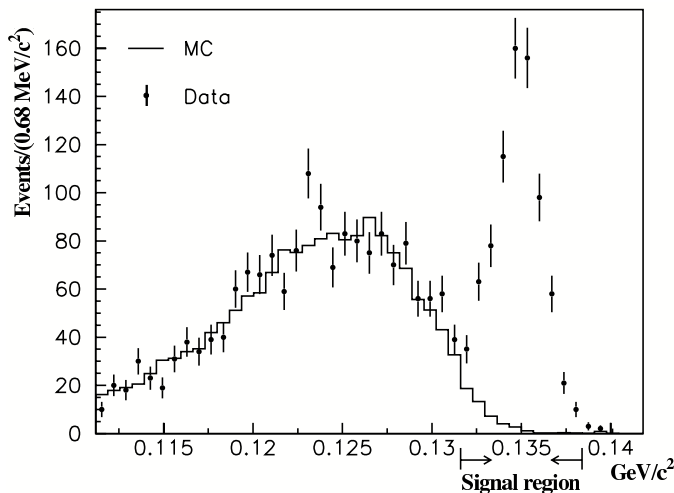


FIG. 3: Positron-electron invariant mass for $\pi^0 \rightarrow e^+e^-$ signal candidates passing all other cuts. The points with error bars are data; the solid histogram is background MC.

Branching ratio uncertainties	
Statistical uncertainty	3.8%
$\pi^0 \rightarrow e^+e^-\gamma$ branching ratio	2.7%
π^0 slope parameter	1.3%
Total external systematic uncertainty	3.0%
Background normalization	1.1%
$m_{e^+e^-}$ resolution	0.7%
Photon pairing χ^2 modeling	0.5%
Kaon momentum spectrum	0.4%
$m_{e^+e^-}$ cutoff in normalization	0.3%
Background MC statistics	0.4%
Signal/normalization MC statistics	0.3%
Total internal systematic uncertainty	1.6%
Total systematic uncertainty	3.4%
Total uncertainty on $B(\pi^0 \rightarrow e^+e^-)$	5.1%

TABLE I: List of uncertainties in the $\pi^0 \rightarrow e^+e^-$ branching ratio.

ture if the branching ratio of the Dalitz decay and the fraction of the decay in the high- x_D region of phase space are measured more precisely. The Dalitz branching ratio used was $B(\pi^0 \rightarrow e^+e^-\gamma) = (1.198 \pm 0.032)\%$ where the relative error, 2.7%, transfers directly into the $\pi^0 \rightarrow e^+e^-$ branching ratio. The MC based on Ref. [16] was used to determine the fraction of Dalitz events that had $m_{e^+e^-} > 65$ MeV/ c^2 , and this number depended on the π^0 form factor used. The result was $\Gamma(m_{e^+e^-} > 65 \text{ MeV}/c^2)/\Gamma(\text{all Dalitz}) = 0.0319$ when using the 2004 PDG[17] average for the π^0 form factor slope. The slope value is dominated by a measurement in a region of spacelike momentum transfer [18] where an extrapolation using vector meson dominance was done. Our observed $m_{e^+e^-}$ distribution disagreed with MC at

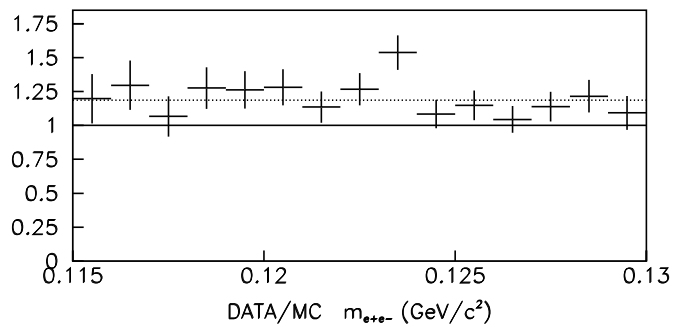


FIG. 4: Ratio of data to MC distribution of $m_{e^+e^-}$ in the sideband region below the signal peak, where the MC was normalized to the number of fully-reconstructed Dalitz decays. The dotted line indicates the ratio over the entire region.

the 1.8σ level and indicated a value that would change the fraction of events in the $m_{e^+e^-} > 65$ MeV/ c^2 tail by 1.3%. This disagreement is quoted here as a systematic error. The detector acceptance depended negligibly on the form factor.

The remaining systematic errors were internal to the experiment. The combination of charged and neutral information in calculating the decay vertex caused a small shift in the $m_{e^+e^-}$ distribution, with the data moving by 0.2 MeV/ c^2 more than the MC. The signal region in data was shifted accordingly to compensate, and an uncertainty in the signal acceptance and the background estimate was a consequence. The shift changed the acceptance by 0.4% and the background estimate by 10.9%. The two errors combined into a 0.7% bias on the branching ratio, which was taken as a systematic error.

A systematic error was associated with the choice of normalization for the background. Normalizing the prediction to the number of fully-reconstructed Dalitz decays resulted in an estimate of 44.4 ± 2.7 background events in the signal region, where the error is from MC statistics only. However, the data indicated a clear excess of events in the sideband region, $110 < m_{e^+e^-} < 130$ MeV/ c^2 , over this Dalitz-normalized MC. The overall level of background had to be scaled up by a factor of 1.19 ± 0.04 (1.24 in the 1997 data; 1.15 in the 1999 data) to match the data. The relative excess showed little $m_{e^+e^-}$ dependence (see Fig. 4). There was no excess of events in the sideband above the signal peak, which might have indicated an unsimulated flat continuum background. The source of the low- $m_{e^+e^-}$ sideband excess was not fully understood, but was likely related to modeling of the sensitivity of the veto system and CsI to the soft photon from high- x_D Dalitz decays. The entire shift was taken as a conservative systematic error. This contributed a 1.1% systematic uncertainty to the branching ratio. The final background estimate was 52.7 ± 11.2 .

The high tail of the pairing χ^2 distribution was not simulated perfectly in the normalization and was a source of systematic uncertainty. Removing the χ^2 cut in the

normalization analysis changed the measured number of decaying kaons by 0.5%. This was not expected to cancel in the ratio, as the pairing χ^2 distributions were different between signal and normalization due to the presence of an additional photon in the normalization sample. The entire sensitivity of the normalization level to the cut was taken as a systematic error.

The simulated kaon momentum distribution deviated from the data, as evidenced by a slope in the ratio of the reconstructed momentum distributions in data and MC. Each MC event was reweighted to account for the slope in both signal and normalization. This modification changed the ratio of signal to normalization acceptances by 0.4%, which was taken as a systematic error on the branching ratio. In the normalization, the cut on $m_{e^+e^-}$ caused a small bias in the branching ratio due to modeling of the acceptance near the $m_{e^+e^-} = 70 \text{ MeV}/c^2$ boundary. Tightening the cut by $5 \text{ MeV}/c^2$ produced a 0.4% difference in the branching ratio.

IV. RESULTS AND CONCLUSION

The final branching ratio was calculated from 794 candidate signal events with an estimated background of 52.7 ± 11.2 , and 1 874 637 normalization events with negligible background. We found

$$\frac{\Gamma(\pi^0 \rightarrow e^+e^-, x_D > 0.95)}{\Gamma(\pi^0 \rightarrow e^+e^-\gamma, x_D > 0.232)} = (1.685 \pm 0.064 \pm 0.027) \times 10^{-4} \quad (3)$$

where $x_D = 0.232$ corresponds to $m_{e^+e^-} = 65 \text{ MeV}/c^2$. Extrapolating the Dalitz branching ratio to the full range

of x_D yields

$$B(\pi^0 \rightarrow e^+e^-, x_D > 0.95) = (6.44 \pm 0.25 \pm 0.22) \times 10^{-8}. \quad (4)$$

In both cases the first error is from data statistics alone and the second is the total systematic error.

Comparison with theoretical predictions and the unitary bound can be done only if we remove the effects of final state radiation. This was done by extrapolating the full radiative tail beyond $x_D = 0.95$ and scaling the result back up by the overall radiative correction of 3.4% to find the lowest-order rate for $\pi^0 \rightarrow e^+e^-$. We found $B^{\text{no-rad}}(\pi^0 \rightarrow e^+e^-) = (7.48 \pm 0.29 \pm 0.25) \times 10^{-8}$, more than seven standard deviations higher than the unitary bound. The result falls between VMD [6] and χ PT predictions [8], with a significance on the difference of 2.3 and 1.5 standard deviations respectively.

Acknowledgments

We gratefully acknowledge the support and effort of the Fermilab staff and the technical staffs of the participating institutions for their vital contributions. This work was supported in part by the U.S. Department of Energy, The National Science Foundation, The Ministry of Education and Science of Japan, Fundação de Amparo a Pesquisa do Estado de São Paulo-FAPESP, Conselho Nacional de Desenvolvimento Científico e Tecnológico-CNPq and CAPES-Ministerio da Educação.

-
- [1] A. Alavi-Harati *et al.*, *Phys. Rev. Lett.* **83**, 922 (1999).
 - [2] S. Drell, *Nuovo Cim.* **XI**, 693 (1959).
 - [3] L. Bergström *et al.*, *Phys. Lett.* **126B**, 117 (1983).
 - [4] L. Bergström, *Z. Phys.* **C20**, 135 (1983).
 - [5] S. Berman and D. Geffen, *Nuovo Cim.* **XVIII**, 1192 (1960).
 - [6] L. Ametller, A. Bramon, and E. Masso, *Phys. Rev.* **D48**, 3388 (1993).
 - [7] M. Savage, M. Luke, and M. Wise, *Phys. Lett.* **B291**, 481 (1992).
 - [8] D. Gomez Dumm and A. Pich, *Phys. Rev. Lett.* **80**, 4633 (1998).
 - [9] M. Knecht *et al.*, *Phys. Rev. Lett.* **83**, 5230 (1999).
 - [10] J. Fischer *et al.*, *Phys. Lett.* **73B**, 364 (1978).
 - [11] J. S. Frank *et al.*, *Phys. Rev.* **D28**, 423 (1983).
 - [12] C. Niebuhr *et al.*, *Phys. Rev.* **D40**, 2796 (1989).
 - [13] A. Deshpande *et al.*, *Phys. Rev. Lett.* **71**, 27 (1993).
 - [14] K. S. McFarland *et al.*, *Phys. Rev. Lett.* **71**, 31 (1993).
 - [15] G. E. Graham, Ph.D. dissertation, The University of Chicago (1999).
 - [16] K. O. Mikaelian and J. S. Smith, *Phys. Rev.* **D5**, 1763 (1972).
 - [17] S. Eidelman *et al.*, *Phys. Lett.* **B592**, 1 (2004).
 - [18] H. Behrend *et al.*, *Z. Phys.* **C49**, 401 (1991).